Available online at www.sciencedirect.com

ScienceDirect

Journal of Electrical Systems and Information Technology 3 (2016) 217–229

www.elsevier.com/locate/jesit

Experimental evaluation of 8 kW grid-connected photovoltaic system in Egypt

A. Elkholy [a,*], F.H. Fahmy [a], A.A. Abou El-Ela [b], Abd El-Shafy A. Nafeh [a], S.R. Spea [b]

[a] *Photovoltaic Cells Department, Electronics Research Institute, Giza, Egypt*
[b] *Electrical Engineering Department, Faculty of Engineering, Menoufiya University, Egypt*

Received 17 May 2015; received in revised form 19 September 2015; accepted 19 October 2015
Available online 2 August 2016

Abstract

An experimental observation study of 8 kW grid-connected photovoltaic (PV) system that is installed at Electronics Research Institute (ERI), Giza, Egypt (Latitude 30.04°N, Longitude 31.21°E), is presented. This study includes the quality of the electrical power generated and injected into the network. The considered system consists of 28 × 295 Wp multicrystalline PV modules, StecaGrid three-phase 8 kW grid-connected inverter and a Solar-Log 300 PM+ for data acquisition and remote monitoring. The power quality parameters at the inverter output side have been measured using CA8335 power quality analyzer. The system has been installed in August 2014 and generated 5.7 MWh till February 2015. The produced electricity by the system is injected directly into the grid without storage device. The purpose of this paper is to present and evaluate the measurements of the power quality parameters obtained from the PV site. Also, this paper presents a comprehensive evaluation of the performance of the system over a period of one week. The observation and analyses exploitation of the collected data can help to evaluate the performance of the PV system connected to the network.

Keywords: Grid-connected photovoltaic system performance; Monitoring PV system; Power quality; Inverter efficiency

1. Introduction

In the power systems, it is very important to find the parameters of the inverter for the photovoltaic (PV) system in order to estimate the efficiency and the power quality improvement. PV technology provides an attractive method of power generation and meets the criteria of clean energy and sustainability (Roscia and Zaninelli, 2002; Tomita, 2005; Heskes and Eslin, 2003; Barker, 2004). Advanced research is still in progress to increase the efficiency of PV cells and optimize the production of energy through the minimization of power losses and better utilization of incident

* Corresponding author.
E-mail address: elkholy.aly@gmail.com (A. Elkholy).
Peer review under the responsibility of Electronics Research Institute (ERI).

Production and hosting by Elsevier

http://dx.doi.org/10.1016/j.jesit.2015.10.004

solar irradiance (Patsalides et al., 2007). The efficiency and proper operation of photovoltaic systems are dependent on a number of factors. Environmental conditions as well as system design constitute the most important factors in the operation of the PV systems and these can have a significant impact on the efficiency and power quality response of the whole system (Patsalides et al., 2007; Aktas et al., 2013; Drews et al., 2008). The variable power flow due to the fluctuation of solar irradiance, temperature and choice of power semiconductor devices are some of the parameters that affect the power quality of the grid-connected PV systems. Good power quality translates into obtaining a sinusoidal voltage and current output from the photovoltaic system; in order to avoid harmonics, interharmonics and eventually voltage distortion (Patsalides et al., 2007; Balcells et al., 2004).

The installed amount of PV systems in distribution systems is expected to grow and it could become comparable with the power supplied by the main source. Therefore, PV systems could have serious consequences on important technical aspects such as quality of the power supplied to customers by utilities, power control, utility protection schemes and islanding operation of the PV systems. In practice, the utility regulations dictate that PV systems should operate at a power factor greater than 0.85 (leading or lagging), when output is greater than 10% of rating (Drews et al., 2008; Balcells et al., 2004; Bouchakour et al., 2012). The maximum grid-connecting frequency deviation is set to be ±0.49 Hz according to national standards of power quality. The islanding detection offset frequency is also in this range (Hussin et al., 2013). Thus, the power quality caused by a large penetration of PV grid-connected systems becomes an important issue (Bouchakour et al., 2012).

The main objective of the PV grid-connected system is to generate the greatest quantity possible of energy. Consequently, the energy production of the photovoltaic systems is the parameter that judges the efficiency of these systems. The purpose of this paper is to present and evaluate the measurements based on power quality quantities which are obtained from the PV grid-connected system site. The measured power quality parameters at the inverter output side are apparent, active and reactive powers, current, voltage and power factor. The total harmonic distortion (THD) for the voltage and current has also been measured as well, over a period of one week. The analysis of measurements reveals the good relation between power quality injected into the network and solar irradiance. Also, this paper presents a comprehensive evaluation of the performance and the efficiency of the system over a period of one week.

2. Grid connected photovoltaic system description

A 8.25 kW peak (KWp) grid-connected PV power generation system was assembled with support from the Photovoltaic Cells Department of Electronics Research Institute (ERI), Giza, Egypt. The terminals of the PV panels that are installed on the rooftop are made available for connection in the laboratory. The DC-side of three-phase 8 kW grid connected inverter is connected to the PV array. The system is designed to inject the generated power directly to the electric grid (Elkholy et al., 2014). The considered system consists of 3 main parts that are solar PV power panels, grid-connected inverter and monitoring system.

2.1. Solar PV power panels

The grid-connected PV system includes 28 multicrystalline modules covering a total area of 54 m^2 with an installed capacity of 8.25 kWp. The system is organized in two sub-arrays, each one is built interconnecting 14 modules in series. Fig. 1 shows photo of the PV power panels involved in this study. The specifications of each PV module are summarized in Table 1. The nominal power of the PV sub-array is around 4.13 kWp, 630 Vdc for nominal voltage.

Table 1
PV module specifications at standard test conditions (STC).

TRINA PV module TSM-295 PC14	
Peak power (P_{max})	295 Wp
Maximum power voltage (V_{mp})	36.6 V
Maximum power current (I_{mp})	8.07 A
Open circuit voltage (V_{oc})	45.2 V
Short circuit current (I_{sc})	8.55 A
Module efficiency (η_m)	15.2%

Fig. 1. Photo of the installed PV array at roof top of ERI site.

2.2. Grid-connected inverter

The output terminals of the solar PV power panels are connected to a StecaGrid 8000+ 3ph grid-connected inverter. This inverter is turned on all the day time and automatically synchronize to the electric grid. If the electric grid has a problem like shut-down or unusual problem, the inverter stops its operation for operator safety (Aktas et al., 2013). Table 2 shows the StecaGrid 8000+ 3ph grid-connected inverter parameters. The electrical data are measured by measurement function of the inverter. Fig. 2 shows a photo of the considered inverter. This inverter shows on its screen the PV system power transmitted to the electric grid, system voltage, amount of produced energy during the day and total run time, etc.

Table 2
Grid-connected inverter specifications.

DC side (PV generator connection)	
Maximum input voltage (VDC_{max})	845 V
Rated input voltage	(350–600) V
AC output side (mains grid connection)	
Rated output voltage	380 V
Rated output current	11.6 A
Rated output power	8000 W
Max. apparent power ($\cos \varphi = 0.90$)	9780 VA
Grid frequency	47.5–52 Hz
Power factor $\cos \varphi$	0.90 (lead-lag)
Maximum efficiency	96.3%

Fig. 2. Photo of the considered inverter.

Since the array voltage and current vary considerably depending upon the weather conditions, the inverter needs to move its working point in order to function optimally. In order to feed the maximum power into the electricity grid, the inverter must work at the maximum-power point (MPP) of the PV array. The MPP tracker ensures that the inverter is adjusted to the MPP point and the greatest possible power is fed into the mains electricity grid.

Fig. 3. Photo for the used monitoring and data acquisition system.

2.3. Monitoring and data acquisition system

Fig. 3 shows a photo for the used monitoring and data acquisition system. It consists, as shown, from the power quality analyzer CA9335 and the Solar-Log 300 (WiFi and PM+ Power Management). All real-time (electrical and meteorological) data are logged into this monitoring system. The grid-connected inverter is connected with the Solar-Log via RS485 interface. The Solar-Log can access the internet via network connection. A Sensor box is connected to the Solar-Log using the RS485 interface. This Sensor box is used to record the meteorological data generated by all the sensors such as solar irradiance, ambient temperature, module temperature and wind speed. The sensor box is installed to be with the same alignment and inclination of the used PV modules (Hussin et al., 2012).

3. Single line diagram

The 8 kW PV array is divided into two strings with an average PV output voltage 500 V. the outputs of the two strings are pooled in the array junction box through DC breakers. A surge protector is incorporated in the system for transient protection and as DC disconnect switch. the output of the array is brought to control room, where the DC power is fed to the power conditioning unit. The 8 kW SecaGrid inverter, that includes filters, maximum power point tracking and control unit, is used to convert the DC PV power into AC power (three phase-four wire), 380 V, 50 Hz and to synchronize it with the grid. The output voltage and frequency of the inverter can follow the grid voltage and frequency during its normal operation. A single line diagram of the set-up grid-connected system is shown in Fig. 4. As shown in this figure, the PV power quality monitoring system is set around the power quality analyzer CA8335. This analyzer is designed as a universal meter for the entire field of power electronics and network analysis. It can be used practically in all power electronics applications, systems testing, and quality assurance. It can be used for measurements in motors,

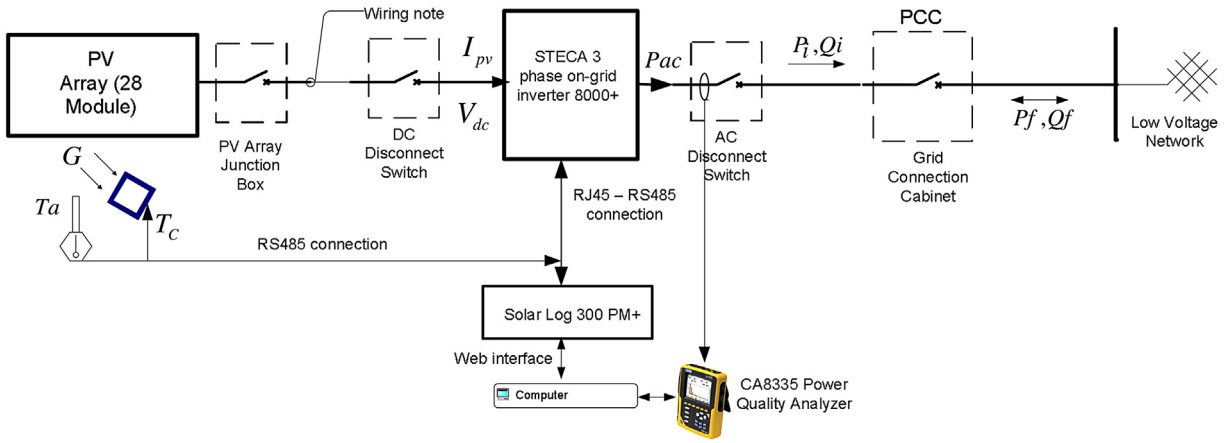

Fig. 4. The single line diagram of the grid connected PV system.

transformers, conventional and switched power supply units. The monitored results are collected using 1 s step. The recorded data are exported and averaged every 5 min and stored in hard disk for analysis and evaluation.

4. Performance analysis methodology

The following parameters are measured; the electrical parameters recorded by the solar-log which located in the control room involves DC/AC voltage, current, power and energy production. Also, the meteorological parameters such as the incident global irradiance in the array plane and module temperature via monocrystalline sensor box and ambient temperature using PT1000. The parameters being monitored are shown in Table 3.

The instantaneous values of all parameters are calculated by normalizing the corresponding energy values (yields and losses) to the recording period over which the recorded samples have been averaged. Physically, they are averages over the recording period, which approximate the instantaneous values. The shorter the recording period, the better is the approximation. In practice, these data are usually treated as instantaneous values and they reflect irradiance and power rather than irradiation or energy (Woyte et al., 2014).

Efficiency of the solar inverter can be defined in two ways. The first approach is based on the values of electrical DC power delivered to the inverter from PV generator (P_{DC}) and the AC power obtained from inverter (P_{AC}). The instantaneous inverter efficiency (η_{inv}) is defined as the ratio of output to input power (Piotrowicz and Maranda, 2013):

$$\eta_{inv} = \frac{P_{AC}}{P_{DC}} \tag{1}$$

The PV array efficiency (η_{PV}) is calculated as:

$$\eta_{PV} = \frac{P_{DC}}{G \times A_a} \tag{2}$$

Table 3
Monitoring parameters of the system.

Electrical measurements	Meteorological measurements
DC current (A), DC voltage (V)	Irradiance, G (W/m^2)
DC power, Pdc (W)	Solar radiation (kWh/m^2)
Output energy, EA (kWh)	Ambient temperature, Ta (°C)
AC active power, Pac (W)	Module temperature, Tc (°C)
Reactive power (var)	
Power factor	
Output rms voltage (V) and current (A)	
Output THD voltage and current (%)	

where A_a is the total active area of PV array, m^2.

G is total in-plane irradiance, kW/m^2.

The instantaneous reference yield (y_r), which is the ratio of the total irradiance (G (kW/m^2)) to the reference irradiance ($G_{stc} = 1$ kW/m^2), is given by Woyte et al. (2014):

$$y_r = \frac{G}{G_{stc}} \tag{3}$$

While, the instantaneous array yield (y_A), which is the ratio of the PV array output power (P_{DC}) to the peak power ($P_{max,stc}$) of the installed PV array (Kymakis et al., 2009).

$$y_A = \frac{P_{DC}}{P_{max,stc}} \tag{4}$$

The instantaneous final yield (y_f), which is the ratio of the net output power of the PV system to the peak power ($P_{max,stc}$) of the installed PV array. The instantaneous final yield can be calculated as follows (Hussin et al., 2013);

$$y_f = \frac{P_{AC}}{P_{max,stc}} \tag{5}$$

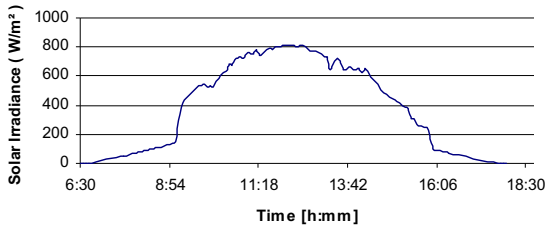

(a) Solar irradiance

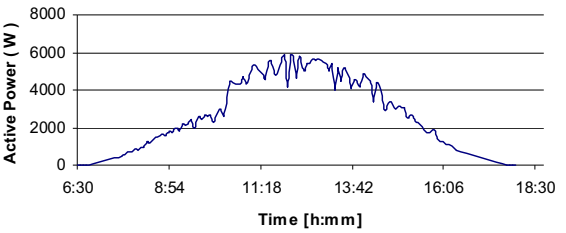

(b) Active power

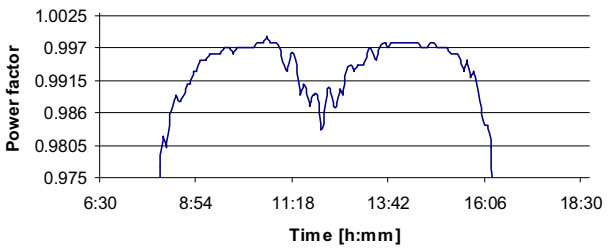

(c) Power factor

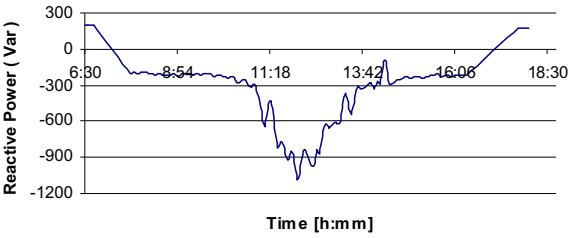

(d) Reactive power

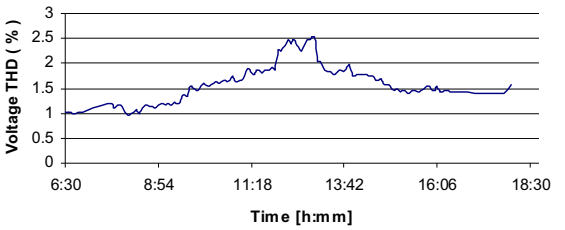

(e) Voltage THD

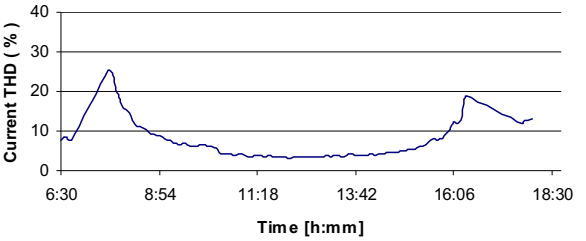

(f) Current THD

Fig. 5. Power quality measurements for a sunny day (5th of February, 2015).

The performance ratio is used to assess the quality of PV installation which is widely reported on a daily, monthly and yearly basis. the instantaneous performance ratio (p_r), is expressed in percentage to describe the overall losses of the PV system output and can be defined by the following equation as (Hussin et al., 2013);

$$p_r = \frac{y_f}{y_r} \tag{6}$$

5. Results and discussion

5.1. Power quality of 8 kW system output

Power quality parameters are measured for the output of the installed PV system at the considered site and correlated to the solar irradiance data that are obtained from the same site. The power quality parameters recorded are the apparent power, active power, reactive power, voltage and current. The power factor and total harmonic distortion for voltage and current are measured as well over a period of one week. The solar irradiance incident on the PV modules is also measured for the test period. Two cases of "sunny" and "cloudy" days are extracted from one week measurement data.

The first examined case is for the sunny day: a typical example of the solar irradiance measurements for a sunny day in February 2015 is shown in Fig. 5(a). The active power produced by the system (Fig. 5(b)) is strongly dependent

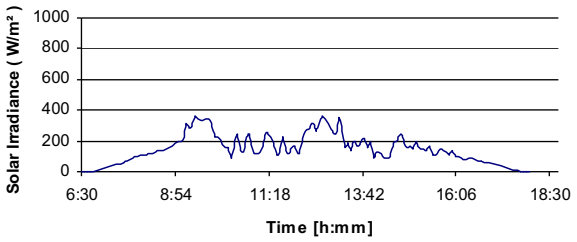

(a) Solar irradiance.

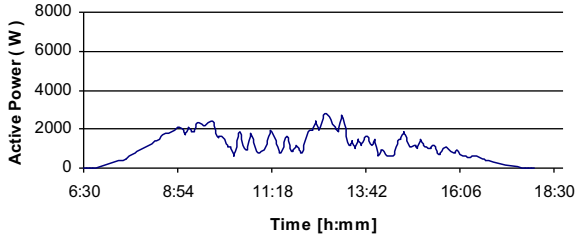

(b) Active power.

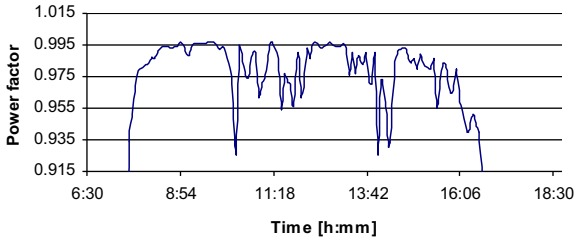

(c) Power factor.

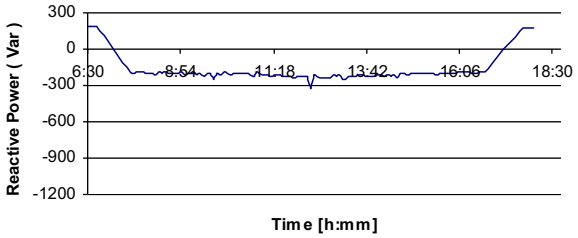

(d) Reactive power.

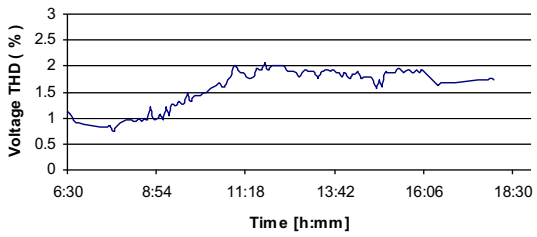

(e) Voltage THD.

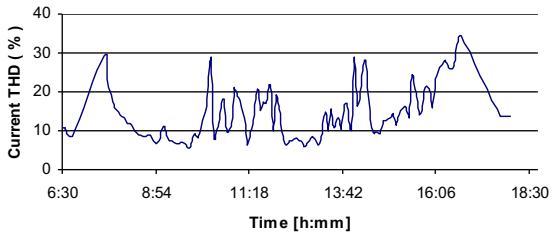

(f) Current THD.

Fig. 6. Power quality measurements for a cloudy day (11th of February, 2015).

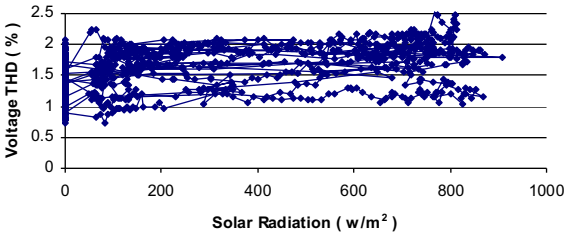

(a) Voltage THD versus solar irradiance

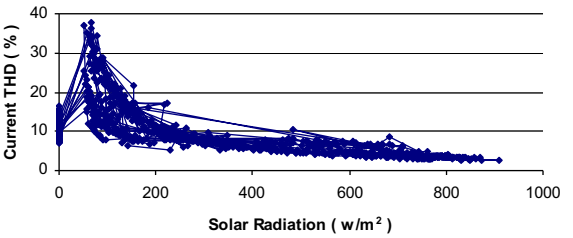

(b) Current THD versus solar irradiance

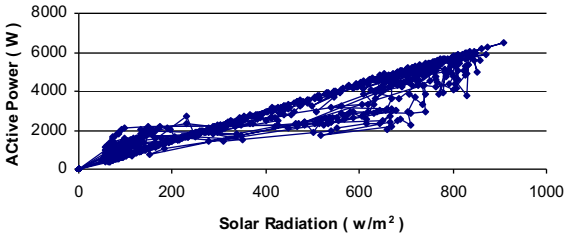

(c) Active power versus solar irradiance

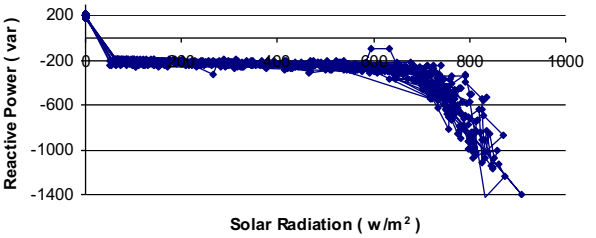

(d) Reactive power versus solar irradiance

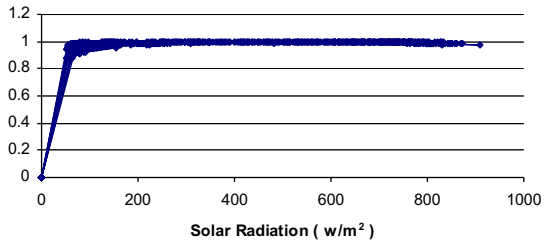

(e) Power factor versus solar irradiance

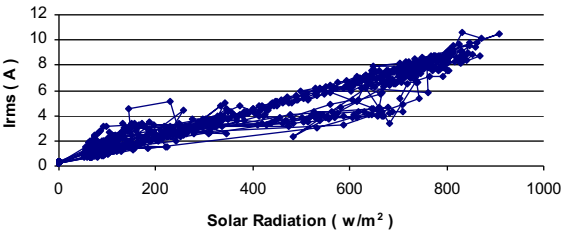

(f) RMS current versus solar irradiance

Fig. 7. Power quality measurements versus solar irradiance.

on solar irradiance. Fluctuations of solar irradiance lead to fluctuations of active power supplied to the distribution network. The unpredictable response of the system, assuming high densities of photovoltaic systems connected to the distribution network, can be troublesome for the producer of energy that has already scheduled the load for the time of peak demand.

The reactive power, as shown in Fig. 5(d) is dependent on the active power of the inverter, maintaining the power factor to the accepted levels as seen in Fig. 5(c) which in turn is affected by solar irradiance levels. from the beginning of its operation and till 11:00 am, the inverter consumes constant low value of reactive power. However, when the active power is greater than 50% of Pnom, it consumes high values of reactive power according to German grid code (VDE AR N4105 and VDE 0126-1-1). The peak reactive power consumed by the considered PV system of a day peak power 6 kWp is about 1 kVar. This is due to the integrated control of the reactive power in the used inverter. Where, modern intelligent inverter designs are now beginning to consider the issue of the reactive power control by providing better compensation based on system parameters and the needs of the distribution network. Voltage and current THDs are shown in Fig. 5(e) and (f), respectively. As can be seen the voltage THD is within 1–2.5%, whereas the current THD increases significantly at low solar irradiance conditions in sunrise and sunset reaching a value of 25% at some instances.

The second examined case is the cloudy day: power quality quantities are measured and the results are presented in Fig. 6. Low solar irradiance can dramatically affect the output of the photovoltaic system as depicted in Fig. 6(a). The active power production (Fig. 6(b)) becomes comparable to reactive power consumption (Fig. 6(d)). the results of the

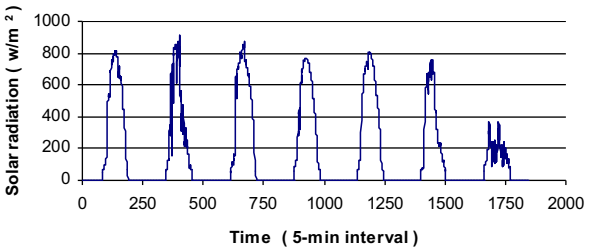

(a) Solar irradiance.

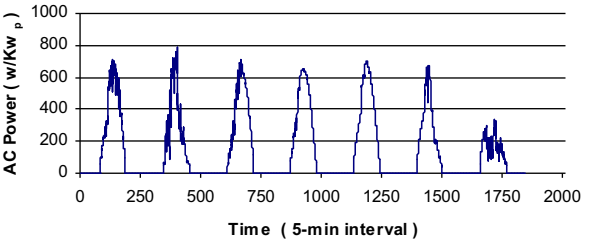

(b) Active power.

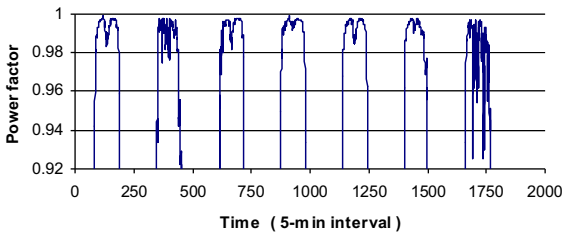

(c) Power factor.

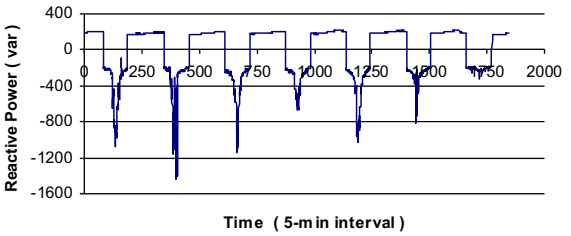

(d) Reactive power.

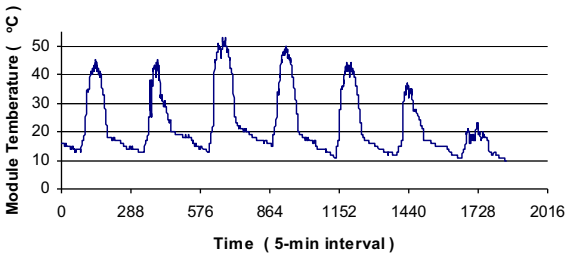

(e) Module temperature.

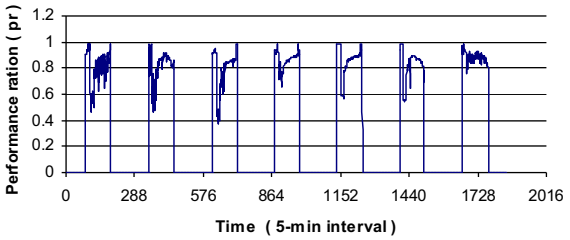

(f) Performance ratio.

Fig. 8. Basic monitored data for one week (5–11 February, 2015).

power factor are found to be acceptable for a large fraction of the day, but it can also be observed that the power factor falls below the acceptable limits during the time of low solar irradiance as shown in Fig. 6(c). The system injects a good power quality to the distribution network during a large fraction of this day and noticed change in power factor cause the changes of solar radiation. Fig. 6(e) shows that, the voltage THD did not exceed 2%. However, the system injects high distorted current to the distribution network during the low solar irradiance conditions as shown in Fig. 6(f).

The last examined case is the power quality quantities which are correlated with instantaneous solar irradiance that is measured during one week. These results are shown in Fig. 7. The voltage and current THDs are shown in Fig. 7(a) and (b), respectively. The voltage THD measured at the output of the system is shown to be not strongly dependent on the fluctuations of solar irradiance (Fig. 7(a)). on the other hand, the current harmonics are very sensitive to changes of incident radiation. These results confirm that the high harmonic content is occurred at the low solar radiation values (Fig. 7(b)). The voltage THD, as shown, is in the range 0.7–2.5%, confirming the existence of an accurate control mechanism for voltage. While, The current THD is indicated to has a large range of values (from 2% to 38%). The active power delivered to the distribution network is found to vary linearly with changes in the solar irradiance incident on the PV modules, as shown in Fig. 7(c). In contrast, the consumed reactive power is dependent on solar irradiance that having higher values beyond 700 W/m^2, because the used inverter is working according to the German grid code (Fig. 7(d)). Finally, the power factor behavior due to changes of solar irradiance is shown in Fig. 7(e). The power factor is shown to act linearly for values of solar irradiance lower than 100 W/m^2 while stays close to unity for the higher

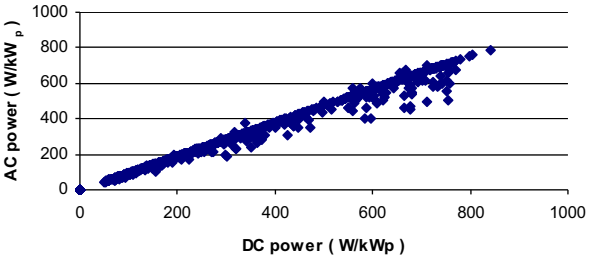

(a) Final yield versus array yield

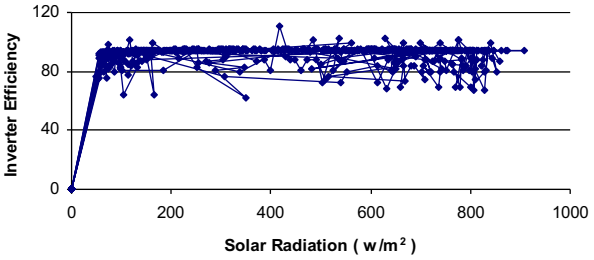

(b) inverter efficiency.

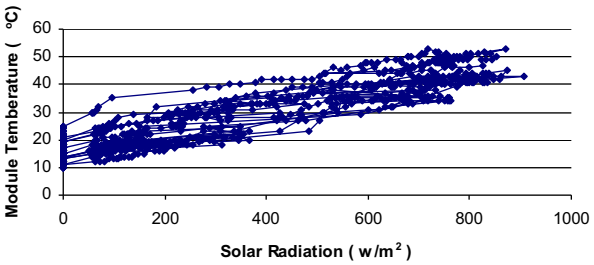

(c) Module temperature.

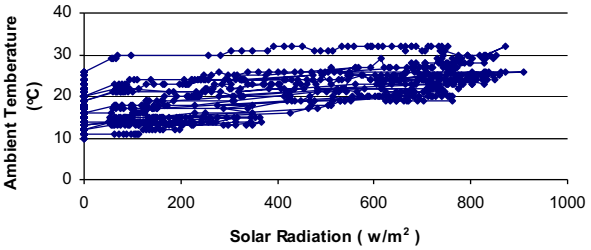

(d) Ambient temperature.

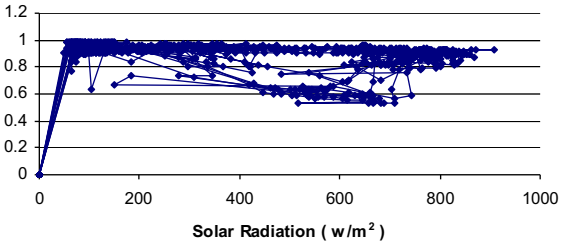

(e) Array Performance (ya)

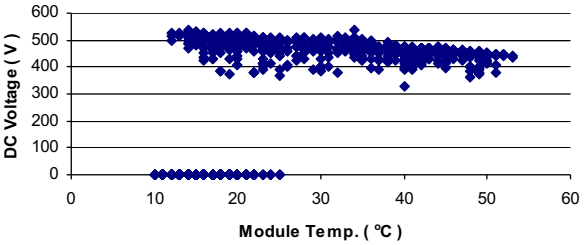

(f) Module temperature versus DC voltage

Fig. 9. Selected relationships of monitoring data using 5-min datasets.

values. The RMS current is shown in Fig. 7(f), and this figure confirms that the RMS current measured at the output of the system, is shown to vary linearly with the changes of solar radiation.

5.2. *Performance analysis and efficiency of the system*

The most straightforward way to rapidly gain first insights is simply visualizing the data as it is recorded, as a function of time. The individual days of the one-week time sequence depicted in Fig. 8. can still be distinguished for each “stamp-plot”, For example it can easily recognize for the last day much lower irradiance and module temperature as shown in Fig. 8(a), (b) and (d) displays the active and reactive power flow for the considered inverter over one-week. Also, Fig. 8(c) shows the power factor over the considered week.

When looking at the detailed shape of the pr (Fig. 8(f)) it can also be recognized a different shape during the third day as compared to the other days, which is formed like a “peak” rather than a “bath-tube”. This well-known “bath-tube” shape of the pr during one entire day which is caused by the increasing of the module temperature. With negative temperature coefficients, the increasing in module temperature causes a reduction of the pr. Consequently, the “bath-tub” shaped profile of the pr is well-pronounced on days with high module temperatures (Fig. 8(e)), which are

clearly related to irradiance intensity: obviously, modules will be warmer under high irradiance as compared with low irradiance intensity.

With many monitoring parameters being related to each other, it becomes clear that scatter plots of two parameters in 2-dimensional Cartesian coordinates can reveal much more information as compared with plotting data over time only, as shown in Fig. 9. The first stamp (Fig. 9(a)) depict final yield versus array yield. The inverter efficiency for the considered measurements period is described in Fig. 9(b). The best result of the maximum inverter efficiency was tracked about 94%. However, the StecaGrid inverter is not operated in excellent performance at certain conditions as indicated by the several scatter data points spreading of events on the plotted graph. This unhealthy condition occurs in winter season and low solar irradiation values.

Fig. 9(c) shows the relation of module temperature with irradiance intensity and with ambient temperature (Fig. 9(d)) and in Fig. 9(e), the array efficiency pr is plotted as a function of irradiation intensity. Finally, Fig. 9(f) explains the operating DC voltage and module temperature. The PV array DC voltage has an inverse relationship with module temperature, the PV array DC voltage falls a little bit because of the temperature coefficient. Other than that, the data point for operating DC voltage was operating safely within the allowable window voltage of the input inverter MPP-voltage limitation. The admissible MPP voltage limit of the inverter in between 350 V and 600 V, meanwhile the maximum input DC voltage about 845 V.

6. Conclusion

The power quality observations obtained from the PV grid-connected system installed in Egypt have been presented. Measurements from the PV array under test have been analyzed and evaluated to observe the overall effect of solar irradiance on the operation of the PV grid-connected system under test. Results for the two different scenarios have been considered, namely, “sunny” and “cloudy” irradiance and the effect of the solar irradiance on the power quality measurements have been investigated. It has been found that a low solar irradiance has a significant impact on the power quality of the output of the PV system. For visual analysis, much information have been already revealed when depicting scatter plots of two measured or derived parameters in two-dimensional Cartesian coordinates. Such a “stamp collection” can reveal interesting details for a given PV installation. As PV module and PV array outputs are degraded on the system performance over the lifetime of the PV system, the designer or planner must be careful to keep the operating array DC voltage matched within the range of the chosen inverter. It’s one of a large series of experimental measurements and analysis of the PV system that must be done to evaluate the general performance and the quality of the electric power generation which is injected to the network.

References

Aktas, Ahmet, Ozdemir, Engin, Karakaya, Abdulhakim, Ucar, Mehmet, 2013. Operation and performance of grid-connected solar photovoltaic power system in Kocaeli University. J. Optelectron. Adv. Mater. 15 (May–June (5–6)), 559–564.

Balcells, J., Dolezal, J., Tlustý, J., Valouch, V., 2004. Impacts of renewable sources on power quality in distribution systems. In: ICEREPQ 04, Barcelona, 31 March–2 April, pp. 5.

Barker, P.P., 2004. Advances in solar photovoltaic technology: an applications perspective. San Francisco, June In: IEEE Power Engineering Society Summer Meeting, vol. 2, pp. 1955–1960.

Bouchakour, S., Cherfa, F., Chouder, A., Abdeladim, K., Kerkouche, K., 2012. Experimental study of grid-connected photovoltaic system at CDER, Algiers. Revue des Energies Renouvelables SIENR’12 Ghardaïa, 59–66.

Drews, A., Beyer, H.G., Rindelhardt, U., 2008. Quality of performance assessment of PV plants based on irradiation maps. Solar Energy 82, 1067–1075.

Elkholy, A., Fahmy, F.H., Abou El-Ela, A.A., El-Shafy, Abd, Nafeh, A., Spea, S.R., 2014. Behavior of 8 kW solar energy unit for reactive power contribution. In: The 8th International Conference on Technology and Sustainable Development in the Third Millennium, Alexandria, Egypt, 22–24 November.

Heskes, P.J.M., Eslin, J.H.R., 2003. Power quality behaviour of different photovoltaic inverter topologies. In: 24th International Conference, Nurnberg, Germany, May, pp. 9.

Hussin, M.Z., Zain, Z.M., Omar, A.M., Shaari, S., 2012. Design installation and testing results of 1 kWp amorphous-silicon FS GCPV system at UiTM, Malaysia. In: IEEE International Conference on Control System, Computing and Engineering, Penang, Malaysia, 23–25 November.

Hussin, M.Z., Omar, A.M., Zain, Z.M., Shaari, S., 2013. Performance of grid-connected photovoltaic system in equatorial rainforest fully humid climate of Malaysia. Int. J. Appl. Power Eng. 2 (December (3)), 105–114, ISSN: 2252-8792.

Kymakis, Emmanuel, Kalykakis, Sofoklis, Papazoglou, Thales M., 2009. Performance analysis of a grid connected photovoltaic park on the island of Crete. Energy Convers. Manage. 50, 433–438.

Patsalides, M., Evagorou, D., Makrides, G., Achillides, Z., Georghiou, G.E., Stavrou, A., Efthimiou, V., Zinsser, B., Schmitt, W., Werner, J.H., 2007. The effect of solar irradiance on the power quality behaviour of grid connected photovoltaic systems. In: International Conference on Renewable Energy and Power Quality (ICREPQ 07), Sevilla, March.

Piotrowicz, Maciej, Maranda, Witold, 2013. Report on efficiency of field-installed PV-inverter with focus on radiation variability. In: 20th International Conference Mixed Design of Integrated Circuits and Systems, Gdynia, Poland, June 20–22.

Roscia, M., Zaninelli, D., 2002. Sustainability and quality through solar electric energy. 10th International Conference on Harmonics and Quality of Power vol. 2, 782–787.

Tomita, T., 2005. Toward giga-watt production of silicon photovoltaic cells, modules and systems. In: 31th IEEE Photovoltaic Specialists Conference, January, pp. 7–11.

Woyte Achim, Richter Mauricio, Moser David, Reich Nils, Green Mike, Mau Stefan, Hassan GL Garrad, Beyer Hans Georg, 2014. Analytical monitoring of grid-connected photovoltaic systems, International Energy Agency Photovoltaic Power Systems Program, IEA PVPS Task 13, Subtask 2 Report IEA-PVPS T13-03, ISBN 978-3-906042-18-3.